# Structural Context of the Great Sumatra-Andaman Islands Earthquake

Michael H. Ritzwoller*, Nikolai M. Shapiro, and E. Robert Engdahl

Center for Imaging the Earth's Interior, Department of Physics,
University of Colorado at Boulder, USA

*To whom correspondence should be addressed; E-mail: ritzwoller@ciei.colorado.edu.

**A new three-dimensional seismic model and relocated regional seismicity are used to illuminate the great Sumatra-Andaman Islands earthquake of December 26, 2004. The earthquake initiated where the incoming Indian Plate lithosphere is warmest and the dip of the Wadati-Benioff zone is least steep along the subduction zone extending from the Andaman Trench to the Java Trench. Anomalously high temperatures are observed in the supra-slab mantle wedge in the Andaman back-arc. The subducting slab is observed along the entire plate boundary to a depth of at least 200 km. These factors contribute to the location of the initiation of rupture, the strength of seismic coupling, the differential rupture speed between the northern and southern segments of the earthquake, and the cause of convergence in the Andaman segment.**

The Great Sumatra-Andaman Islands earthquake with a moment-magnitude of about $M = 9.3$ (*1*) ruptured an area greater than 18000 km$^2$ (*2*) along a 1200 km boundary between the Indian Plate and the Burma Microplate (often considered to be part of the greater Eurasian Plate). The earthquake remains under intense study, but several enigmatic characteristics have come to the fore. First, the earthquake rupture proceeded along two distinct segments with very different rupture speeds. The southern (Sumatran) segment where the rupture originated is characterized by normal rupture speeds (*3*). Tsunami run-up data indicate that most of the tsunami was generated by this "fast" segment (*4*). The northern (Andaman-Nicobar) segment of the rupture, in contrast, released about two-thirds of the total seismic moment (*1*) and had an unusually slow rupture speed. Second, all previous large ($M > 9$) earthquakes have occurred in regions where subduction is largely perpendicular to the trench. Present-day plate models and tectonic reconstructions indicate that the nearly oblique incidence of the Indian and Burma plates (Fig. 1A) has occurred west of the Andaman Sea for at least 20 million years (*5–7*).

The characteristics of this earthquake can be partially understood in terms of surface observables that have revealed its unusual tectonic setting, including the age-variability of the incoming Indian Plate along its subducting edge, the existence of active spreading in the back-arc beneath the Andaman Sea (*8–10*), and anomalously strong strain partitioning (*11, 12*) in which the oblique Sumatra-Andaman subduction is accommodated by strike-slip motion released along the transform Sumatra and Andaman faults that run nearly parallel to the trench. Better understanding of the earthquake will come in part from improved models of the thermal and mechanical structure and variability at depth. To address this issue we have relocated and reviewed modern and historical seismicity and produced a new shear velocity model of the uppermost mantle constructed using broadband seismic surface waves.

To improve knowledge of historical seismicity, all instrumentally recorded earthquakes in the Andaman Islands region that are well constrained by teleseismic observations have been relocated using well established methods (13, 14) with special attention to focal depth. These earthquakes are complete and have been reviewed to magnitude 6.5 for the historical period (pre-1964) and 5.5 for the modern period with a relative location accuracy of about 15 km. Reviewing entails examining the internal consistency of the arrival time data, particularly the depth phases. Well constrained earthquakes less than $M = 5.5$ during the modern period are in the process of being reviewed. Observed seismicity portrays the spatial distribution of interslab and intraslab (deep) earthquakes in the region and the relationship of this seismicity to regional structures (Figs. 2A-C).

Surface waves provide the most uniform coverage of the region of study and observations of surface wave dispersion strongly constrain shear velocities which are related to temperatures in the uppermost mantle (15). Using information about surface wave phase (16, 17) and group (18, 19) speed dispersion across the region we estimated a three dimensional (3-D) tomographic model of shear-wave speed in the Earth's upper mantle on a $1° \times 1°$ grid. The method involves surface-wave diffraction tomography (19) followed by a Monte-Carlo method (20) to estimate both shear velocity and temperature in the upper mantle (21–23).

First, the relocated seismicity and the new model of the seismic and thermal structure of the upper mantle help to understand the location of the initiation of rupture and illuminate why rupture proceeds differently in the southern and northern segments of the fault. These issues are related to the dip angle of the subducting plate and the temperature of the supra-slab mantle wedge. Rupture initiated in northern Sumatra, where the Indian Plate and the supra-slab mantle wedge appear to be very strongly coupled. Slow rupture speeds in the northern segment of the fault are correlated with very high temperatures

3

in the mantle overlying the subducting plate, associated with the Andaman spreading center.

The Indian Plate is believed to be strongly coupled to the mantle wedge in northern Sumatra because the subducting lithosphere is young and is observed to be warm (Fig. 1B, 2B), and because of a more gentle dip in the Wadati-Benioff zone (Fig. 2A-C). Prior to about 40 Ma, India and Australia occupied different plates separated by a spreading center called the Wharton Ridge (*24–26*). After ~40 Ma, Australia rifted from Antarctica, seafloor spreading along the Wharton Ridge ceased, and India and Australia began to move in unison as part of the Australian-Indian Plate. This complex history is apparent in the variation of lithospheric age along the Andaman, Sunda, and Java Trenches (Fig. 1A), with the youngest oceanic lithosphere (Wharton Fossil Spreading Ridge) of about ~40 Ma currently being subducted beneath northern Sumatra (*27*). Significantly older lithosphere is subducting at both the Andaman and Java trenches. The seismically inferred thermal structure of the incoming Indian Plate represents the plate's tectonic history (Fig. 1B). The young apparent thermal age (*23*) approximately follows the Wharton Fossil Ridge with the warmest lithosphere lying somewhat to its north. This may be explained by the influence of the Kerguelen plume (*24*) that caused the delayed thickening of the oceanic lithosphere under the Ninetyeast Ridge (*28*). The location of the thermally warmest and thinnest lithosphere is at the Sunda Trench and nearly coincides with the location of the initiation of rupture of the Great Sumatra-Andaman Islands earthquake. This is probably no mere coincidence, as the warmer subducting lithosphere near the Wharton Fossil Ridge is more buoyant, the slab dips less steeply (Fig. 2B), and hence the coupling to the overlying plate is stronger than beneath the Andaman and Java trenches. The lithosphere approaching northern Sumatra (Fig. 2B) is also observed to be thinner than lithosphere approaching the Andaman and Java Trenches (Fig. 2A,C), and thinner upon

subduction as well. Stronger coupling is also indicated by GPS data ($29$). In addition, the Benioff-Wadati zone in northern Sumatra is less steep than in adjacent areas to the north and south ($\sim30°$ compared with $\sim50°$ and $\sim40°$ to the north and south, respectively), consistent with the thermal state of the incoming lithosphere.

After initiation, the Sumatra-Andaman Islands earthquake ruptured northwestward. The back-arc beneath the Sunda Trench is seismically fast and cool (Fig. 2B), but as rupture progressed mantle wedge temperatures at the rupture increased dramatically (Fig. 2A, 2D). High mantle temperatures may act to slow the rupture. These warm temperatures are consistent with the interpretation of the Andaman Sea as an extensional basin created by rifting over the past 11 Ma ($8–10$) caused by the relative motion of various lithospheric blocks in response to the collision between India and Asia ($9, 30$).

Second, improved knowledge of seismicity and the thermal structure of the upper mantle also illuminate why a great earthquake occurred at a highly oblique plate boundary. Subducting lithosphere is clearly imaged along the entire plate boundary, from the Andaman Trench to the Java trench (Figs. 2A-C, 3) down to at least 200 km depth with well defined Wadati-Benioff zones. Several regional and global P-wave tomographic models ($7, 31–33$) show the trace of subducted oceanic lithosphere at depths larger than 200 km. Centroid-moment-tensor solutions show that thrust earthquakes are common along the Nicobar-Andaman segment of the subduction zone with nearly east-west compression ($8, 34$). Large historical ($M \sim 8$) thrust earthquakes have occurred ($8$) along this segment and GPS data indicate non-negligible east-west convergence ($35$). Convergence must, therefore, be occurring and have occurred well into the past along the entire plate boundary even beneath the most oblique Nicobar-Andaman segment of the plate boundary. This is in striking contrast with the purely transform motion observed in other very oblique segments of subduction zones such as the Western Aleutians ($36$) where a "slab

window" is observed beneath the trench along the highly oblique segment of the plate boundary devoid of both subducting lithosphere and deep seismicity.

The existence of subducting lithosphere along the entire rupture of the great earthquake confirms but does not explain convergence. Convergence may be explained tectonically by strain partitioning in the back-arc of the Sunda Trench in which the lithospheric sliver between the Sunda Trench and the strike-slip Sumatra Fault is conveyed northwestward. Convergence is achieved when this sliver intersects the bend where the Sunda and Andaman trenches meet. Strong coupling produced by the warm incoming lithosphere may enhance strain partitioning inboard of the Sunda Trench with most of strike-slip motion released along the transform Sumatra Fault that runs nearly parallel to the trench. This same northwest motion contributes to the opening of the Andaman Basin and, hence, to convergence. The seismic model suggests another source of convergence. The incoming oceanic lithosphere off the Andaman Basin is very thick and, therefore, negatively buoyant. Oblique incidence at the Andaman Trench poorly couples the Indian Plate with the Burma Microplate. Convergence may, therefore, be enhanced by the weak Andaman lithosphere responding to slab roll-back.

# Competing interests statement.

# References and Notes

1. Stein and Okal, moment-magnitude estimation from the Earth's gravest normal modes is described at :

http://www.earth.northwestern.edu/people/seth/research/sumatra.html

2. http://neic.usgs.gov/neis/eq_depot/2004/eq_041226/

3. The finite fault model is computed by Chen Ji, Caltech, as referenced at:
   http://neic.usgs.gov/neis/eq_depot/2004/eq_041226/neic_slav_ff.html

4. Bilham, R., E.R. Endahl, N. Felfl, and S.P. Satyabala, Partial and complete rupture of the Indo-Andaman plate boundary 1847-2004, *Seism. Res. Lett.* submitted.

5. T.Y. Lee, L.A. Lawver, Cenozoic plate reconstruction of Southeast Asia, *Tectonophysics* **251**, 85-138 (1995).

6. R. Hall, Reconstructing Cenozoic SE Asia. In: Hall, R. and Blundell, D. J. (eds.) Tectonic Evolution of SE Asia. *Geological Society of London Special Publication* **106**, 153-184 (1996).

7. A. Replumaz, H. Karason, R.D. van der Hilst, J. Besse, P. Tapponnier, 4-D evolution of SE Asia's mantle from geological reconstructions and seismic tomography: *Earth Planet. Sci. Lett.* **221**, 103-115 (2004).

8. M. Ortiz, R. Bilham, Source area and rupture parameters of the 31 Dec. 1881 Mw=7.9 Car Nicobar earthquake estimated from Tsunamis recorded in the Bay of Bengal, *J. Geophys. Res.* **108**, , 2215, doi:10.1029/2002JB001941 (2003).

9. K.A.K. Raju, T. Ramprasad, P.S. Rao, B.R. Rao, J. Varghese, New insights into the tectonic evolution of the Andaman basin, northeast Indian Ocean, *Earth Planet. Sci. Lett.* **221**, 145-162 (2004).

10. P.K. Khan, P.P.Chakraborty, Two-phase opening of Andaman Sea: a new seismotectonic insight, *Earth Planet. Sci. Lett.* **229**, 259-271 (2005).

11. R. McCaffrey *et al.*, Strain partitioning during oblique plate convergence in northern Sumatra: Geodetic and seismologic constraints and numerical modeling, *J. Geophys. Res.* **105**, 28,363-28,376 (2000).

12. G. Michel *et al.*, Y. Yu, S. Zhu, C. Reigber, M. Becker, E. Reinhart, W. Simons, B. Ambrosius, C. Vigny, N. Chamot-Rooke, X. LePichon, P. Morgan, S. Matheussen, Crustal motion and block behavior in SE-Asia from GPS measurements. *Earth Planet. Sci. lett.* **187**, 239-244 (2001).

13. E.R. Engdahl, Van der Hilst, R.D., and Buland, R.P., Global teleseismic earthquake relocation with improved travel times and procedures for depth determination: *Bulletin of the Seismological Society of America*, **88**, p. 3295-331 (1998).

14. E.R.Engdahl and A. Villasenor, Global Seismicity: 1900-1999, International Handbook of Earthquake and Engineering Seismology, v. **81A**, Elsevier Science Ltd., Amsterdam, The Netherlands, pp. 665-690, (2002).

15. S. Goes, R. Govers, R. Vacher, Shallow mantle temperatures under Europe from P and S wave tomography, *J. Geophys. Res.* **105**, 11,153-11,169 (2000).

16. J. Trampert, J.H. Woodhouse, Global phase velocity maps of Love and Rayleigh waves between 40 and 150 seconds, *Geophys. J. Int.* **122**, 675-690 (1995).

17. G. Ekström, A.M Dziewonski, *Nature* **394**, 168-172 (1998).

18. M.H. Ritzwoller, A.L. Levshin, Eurasian surface wave tomography: Group velocities, *J. Geophys. Res.* **103**, 4839-4878 (1998).

19. M.H. Ritzwoller, N.M. Shapiro, M.P. Barmin, A.L. Levshin, Global surface wave diffraction tomography, *J. Geophys. Res.* **107**, 2235, doi:10.1029/2002JB001777 (2002).

20. N.M. Shapiro, Ritzwoller, M.H., Monte-Carlo inversion for a global shear velocity model of the crust and upper mantle, Geophys. J. Int. **151**, 88-105 (2002).

21. N.M. Shapiro, Ritzwoller, M.H., Thermodynamic constraints on seismic inversions, *Geophys. J. Int.* **157**, 1175-1188, doi:10.1111/j.1365-246X.2004.02254.x (2004).

22. M.H. Ritzwoller, N.M. Shapiro, S. Zhong, Cooling history of the Pacific lithosphere, *Earth Planet. Sci. Lett.* **226**, 69-84, doi:10.1016/j.epsl.2004.07.032 (2004).

23. The temperature parameterization (*21, 22*) has two principal mantle unknowns.: the "apparent thermal age" of the lithosphere which is the age at which a conductively cooling half-space would match the observed lithospheric temperature structure and the "potential temperature" of the asthenosphere which is the upward continuation to the surface of asthenospheric temperatures following the mantle adiabatic gradient.

24. D. Weis, F.A. Frey, Role of the Kerguelen Plume in generating the eastern Indian Ocean seafloor, *J. Geophys. Res.* **101**, 13,831-13,849 (1996).

25. C. Deplus *et al.*, Direct evidence of active deformation in the eastern Indian Ocean plate, *Geology* **26**, 131-134 (1998).

26. H. Hébert, B.Villemant, C. Deplus, M. Diament, Contrasting geophysical and geochemical signatures of a volcano at the axis of the Wharton fossil ridge (N-E Indian Ocean), *Geophys. Res. Lett.* **26**, 1053-1056 (1999).

27. R.D. Mueller, W.R. Roest, J.-Y. Royer, L.M. Gahagan, J.G. Sclater, Digital isochrons of the world's ocean floor, *J. Geophys. Res.* **102**, 3211 (1997).

28. A. Davaille, J.M. Lees, Thermal modeling of subducted plates: tear and hotspot at the Kamchatka corner, *Earth Planet. Sci. Lett.* **226**, 293-304 (2004).

29. Crustal displacements and deformation pattern in SouthEast Asia, determined by GPS campaigns conducted under the GEODYSSEA (*12*) and SEAMERGES (http://www.deos.tudelft.nl/seamerges/) programs from 1994 to present indicate highly coupled subduction beneath northern Sumatra. This result is presented in a report on the great Sumatra-Andaman Islands earthquake prepared by Christophe Vigny (http://www.geologie.ens.fr/~vigny/aceh-e.html).

30. P. Tapponnier, G. Peltzer, A.Y. Le Dain, R. Armijo, P. Cobbold, Propagating extrusion tectonics in Asia: New insights from simple experiments with plasticine, *Geology* **10**, 611-616 (1982).

31. S. Widiyantoro, R.D. Van der Hilst, Structure and evolution of subducted lithosphere beneath the Sunda arc, Indonesia, *Science* **271**, 1566-1570 (1996).

32. S. Widiyantoro, R.D. Van der Hilst, Mantle structure beneath Indonesia inferred from high-resolution tomographic imaging, *Geophys. J. Int.* **130**, 167-182 (1997).

33. E. Hafkenscheid, S.J.H. Buiter, M.J.R. Wortel, W. Spakman, H. Bijwaard, Modelling the seismic velocity structure beneath Indonesia: a comparison with tomography. *Tectonophysics* **333**, 35-46 (2001).

34. K. Rajendran, H.K. Gupta, Seismicity and tectonic stress field of a part of the Burma-Andaman-Nicobar Arc, *Bull. Seism. Soc. Am.* **79**, 989-1005 (1989).

35. J. Paul *et al.*, The motion and active deformation of India. *Geophys. Res. Lett.* **28**, 647-651 (2001).

36. V. Levin, N.M. Shapiro, J. Park, M.H. Ritzwoller, The slab portal beneath the Western Aleutians, *Geology*, in press.

37. C. DeMets, R.G. Gordon, D.F. Argus, S. Stein, Effect of recent revisions to the geomagnetic reversal time scale on estimates of current plate motions, *Geophys. Res. Lett.* **21**, 2191-2194 (1994).
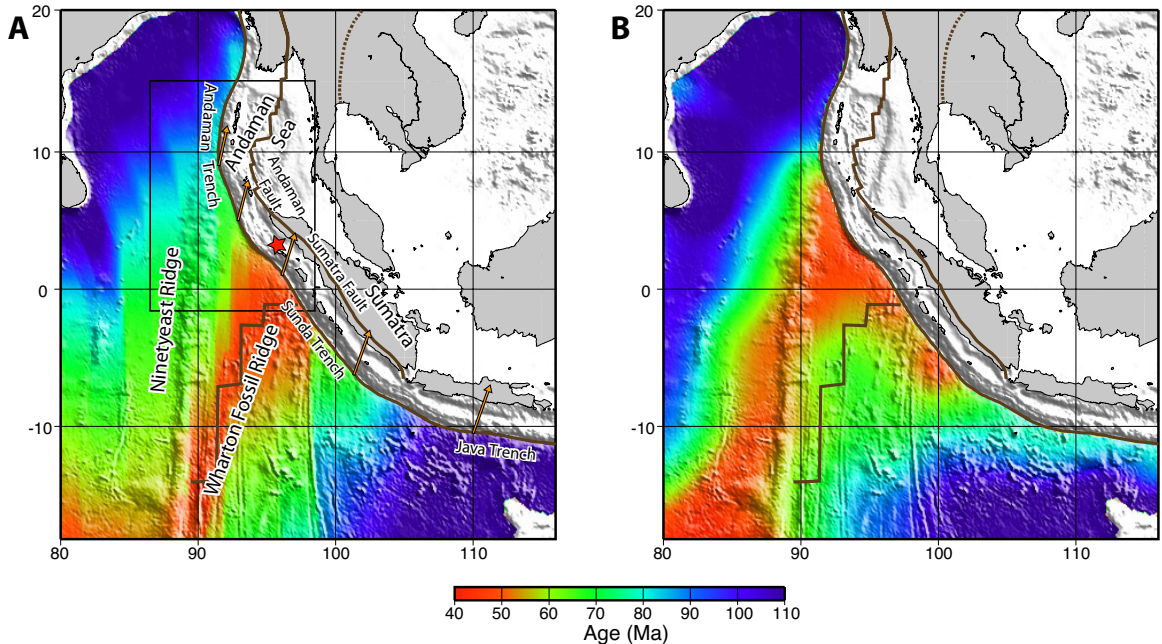
Figure 1: (A) Reference map showing the locations of the principal geographical and geological features discussed in the test. The red star marks the location of the initiation of rupture of the great Sumatra-Andaman earthquake. Brown lines show active and fossil plate boundaries. Arrows show the relative plate motion (*37*). The age of the incoming oceanic plate (*27*) is shown with colors in millions of years. The black rectangular box indicates the region shown in Fig. 3. (B) Distribution of the apparent thermal age which results from the seismic inversion using the thermal parameterization (*21–23*). It is defined as the lithospheric age at which a purely conductive temperature profile would most closely resemble the observed thermal structure.
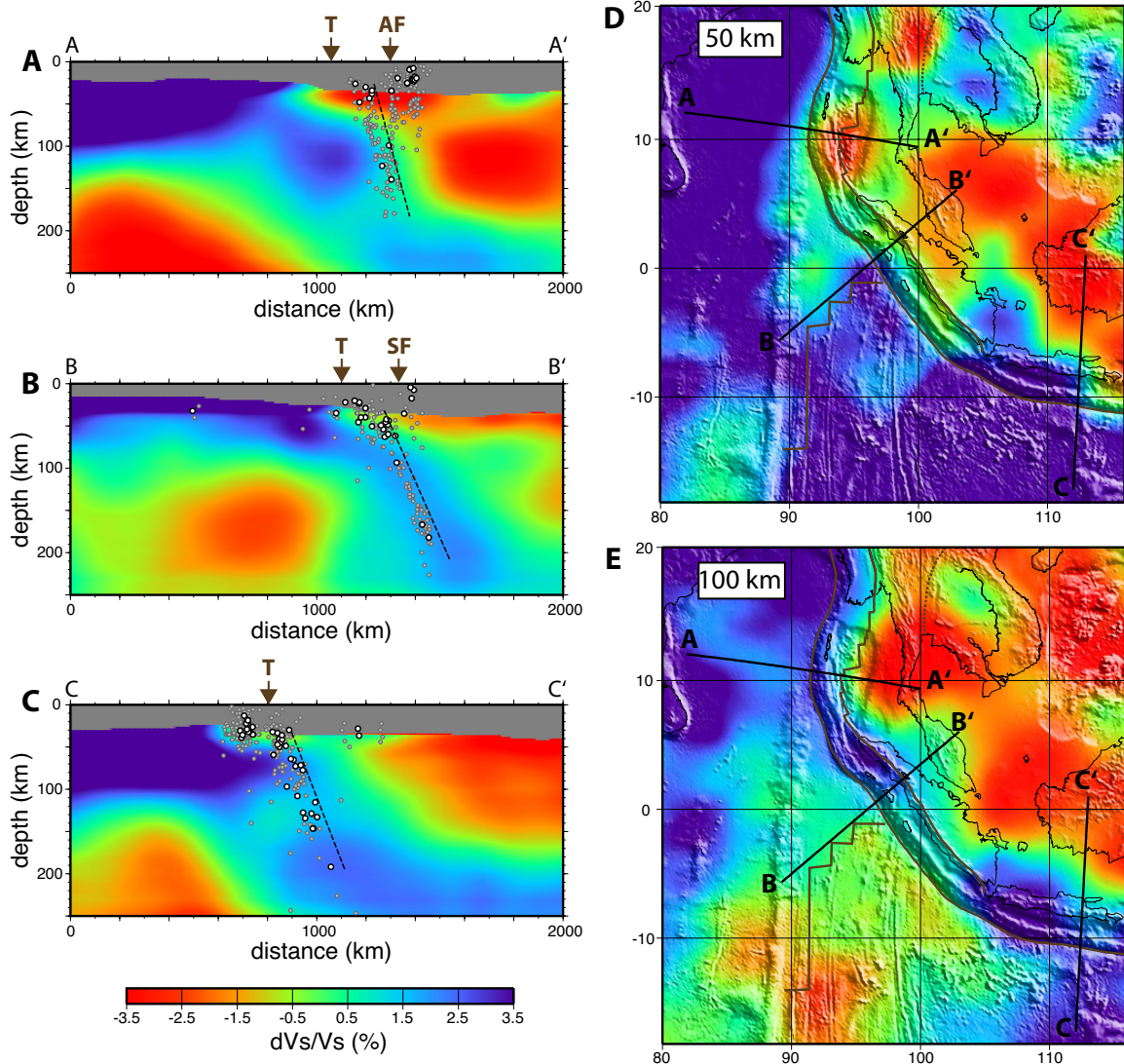
Figure 2: Results of the inversion using the seismic parameterization (*20*). (A-C) Vertical cross-sections through the shear velocity model. Colors indicate anomalies in S-wave velocity relative to a regional one-dimensional profile. The location of the trench and the Sumatra and the Andaman Faults are shown with small arrows on top of the cross-sections. Hypocentres of relocated earthquakes within 100 km of the profile plane are shown by circles. Larger white circles indicate hypocenters that were both relocated and reviewed. Dashed lines show the deduced orientation of the Wadati-Benioff zones. (D) and (E) Horizontal cross-section through the shear velocity model at 50 km and 100 km depths, respectively.

13
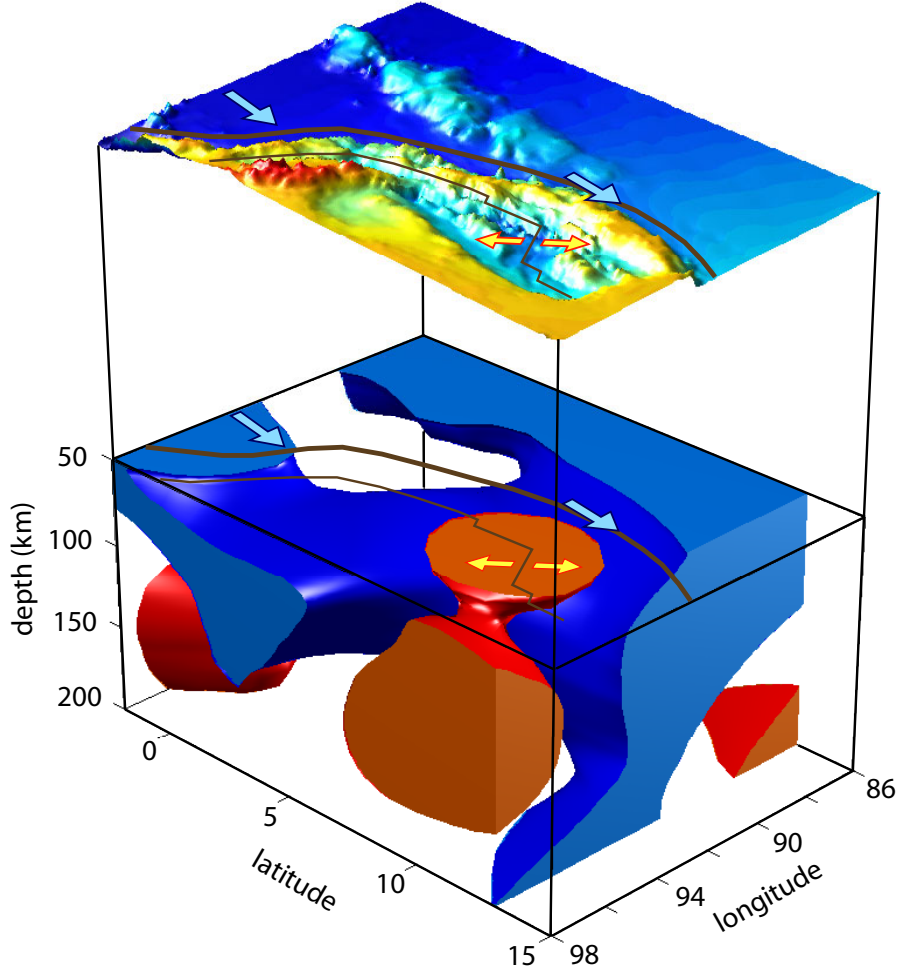
Figure 3: Isosurface representation of the shear velocity model beneath part of northern Sumatra and the Andaman Sea (identified with the black box in Fig. 1), in which the model was laterally smoothed with a gaussian filter ($\sigma = 100$ km) to highlight the dominant large-scale features. The blue surface (+1.2%) represents the high seismic velocity oceanic lithosphere subducting at the Sunda and the Andaman trenches. The gap in the blue surface corresponds to the warmest oceanic lithosphere in vicinity of the Wharton Fossil Ridge and the Nintyeast Ridge. The red surface (-1.5%) reflects low seismic velocity material beneath the Andaman Sea. Vertically exaggerated topography is shown with a colored isosurface on the top. The brown lines show the actice plate boundaries. Blue arrows show relative plate motion and yellow arrows indicate the extension in the Andaman Basin.

14